Journal of Organometallic Chemistry 695 (2010) 249–255

Contents lists available at ScienceDirect

Journal of Organometallic Chemistry

journal homepage: www.elsevier.com/locate/jorganchem

# Synthesis and complexation properties of novel triazoyl-based ferrocenyl ligands

Gilles Gasser [a,b,*], Jonathan D. Carr [b], Simon J. Coles [c], Stephen J. Green [b], Michael B. Hursthouse [c], Sean M. Cafferkey [c], Helen Stoeckli-Evans [a,1], James H.R. Tucker [d,*]

[a] Institute of Chemistry, University of Neuchâtel, Av. de Bellevaux 51, CH-2009 Neuchâtel, Switzerland
[b] School of Chemistry, University of Exeter, Stocker Road, Exeter EX4 4QD, UK
[c] School of Chemistry, University of Southampton, Highfield, Southampton SO17 1BJ, UK
[d] School of Chemistry, University of Birmingham, Edgbaston, Birmingham B15 2TT, UK

ARTICLE INFO

*Article history:*
Received 10 August 2009
Received in revised form 24 September 2009
Accepted 1 October 2009
Available online 12 October 2009

*Keywords:*
Self-assembly
Supramolecular chemistry
[2 × 2] Grids
Ferrocene
N ligands

ABSTRACT

Two new ligand derivatives of ferrocene, namely *N*-4-[3,5-di-(2-pyridyl)-1,2,4-triazoyl]ferrocene carbimine (**L1**) and *N*-4-[3,5-di-(2-pyridyl)-1,2,4-triazoyl]ferrocene carbamide (**L2**), were synthesised in good yields by reacting the known compound 3,5-di-pyridine-2-yl-[1,2,4]triazol-4-ylamine (**1**) with ferrocenecarbaldehyde and chlorocarbonyl ferrocene, respectively. The structures of **L1** and **L2** were determined by X-ray crystallography. The complexation of **L1** and **L2** with $Cu^{I}$, $Ag^{I}$, $Zn^{II}$ and $Cd^{II}$ was studied by NMR and UV–vis spectroscopies, as well as by electrochemistry, with titrations used to determine metal:ligand stoichiometries. The cyclic voltammograms of **L1** and **L2** and their respective complexes indicated reversible one-electron transfers corresponding to the $Fc^{0/+}$ redox couple (Fc = ferrocene), with formal electrode potentials shifting to more positive values upon metal complexation.



## 1. Introduction

The self-assembled formation of well-defined metal-containing architectures is an ongoing topical area in supramolecular chemistry [1,2]. In particular, grid-type coordination arrays, which consist of a regular array of metal cations arranged between two perpendicular sets of parallel ligands, have been extensively studied over the past years [3–6]. The resulting compounds present interesting physico-chemical properties, such as electrochemical [7,8], optical [8], electronic [9], magnetic [10–12] or catalytic activity [13]. The choice of suitable ligands and metal ions is hence crucial for their synthesis. In the case of grids, the ligands used are normally planar and contain rigid linear spacers between the binding sites. The choice of metal ions employed depends on the number and type of coordinative sites of the ligand. Although the properties of self-assembled structures have been examined in detail, electrochemistry has seldom been used to follow their formation. One convenient method for doing this is to simply append or link redox-active units to ligands that can form self-assembled complexes. Previously ferrocene has been utilised as a linker group between bipyridine and quinquepyridine ligands that form helicate complexes with metal ions [14,15]. More recently, the controlled self-assembly of ferrocene-containing heterobimetallic rhomboidal and hexagonal complexes and their associated electrochemistry were reported [16]. Here we report two new ligands (**L1** and **L2**, Scheme 1) bearing a ferrocene (Fc) unit that were designed primarily to investigate the possibility of forming novel redox-active assembled structures and to monitor the formation of these assemblies through electrochemical means. Furthermore, since it has previously been shown that the aggregation of ferrocene-containing surfactants can be controlled using the $Fc^{0/+}$ redox couple [17,18], a secondary aim was to determine whether the strength of these inorganic assemblies could be controlled by the Fc redox state.

As shown by our [19,20] and other more recent [14,21–24] studies on ferrocene-containing metal complexes involving heterocyclic ligands, the ferrocene group is an ideal choice as a redox-active moiety due to the ease in which it can be functionalised with metal-binding ligands and its reversible electrochemistry. The coordinative unit selected for this work was a derivative of 3,5-di-pyridine-2-yl-[1,2,4]triazol-4-ylamine [25,26] (**1**, Scheme 1) and was chosen because tetrahedral complexes of 1:1 stoichiometry were anticipated to be not dissimilar to those obtained by Youinou et al. in [2 × 2] grid formation with 3,6-bis(2′-pyridyl)pyridazine

* Corresponding authors. Present address: Ruhr-University Bochum, Faculty of Chemistry and Biochemistry, Inorganic Chemistry I, Bioinorganic Chemistry, Universitätsstrasse 150, D-44801 Bochum, Germany (G. Gasser). Fax: +49 (0) 234 32 14378 (G. Gasser); +44 (0) 121 414 4403 (J.H.R. Tucker).
*E-mail addresses:* gilles.gasser@rub.de (G. Gasser), helen.stoeckli-evans@unine.ch (H. Stoeckli-Evans), j.tucker@bham.ac.uk (J.H.R. Tucker).
[1] Present address: Institute of Physics, University of Neuchâtel, rue Emile-Argand 11, CH-2009 Neuchâtel, Switzerland. Fax: +41 (0) 32 718 25 11.

0022-328X/$ - see front matter © 2009 Elsevier B.V. All rights reserved.
doi:10.1016/j.jorganchem.2009.10.004

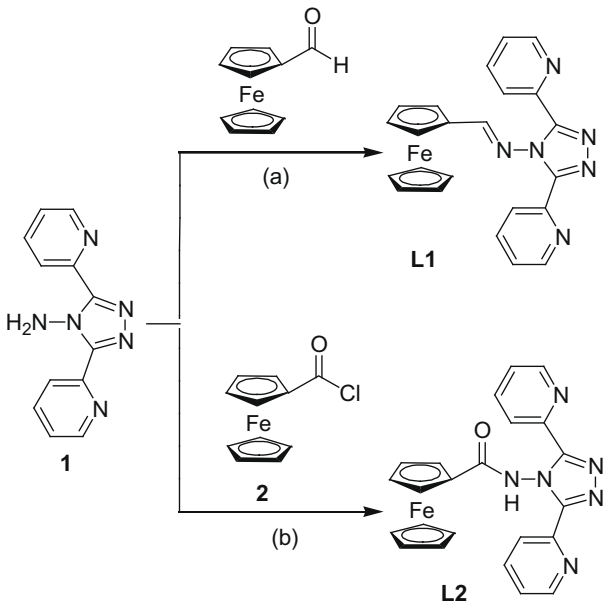


**Scheme 1.** Synthesis of **L1** and **L2**. (a) $H_2SO_{4conc.}$, 5 Å molecular sieves, toluene, reflux, 22 h, 56%. (b) Triethylamine, $CH_2Cl_2$, 0 °C to r.t., 64 h, 59%.

[27]. Ligand **1** also presents the advantage of having a free amino group, which can be easily coupled to the ferrocene group in different ways.

Multinuclear complexes of $Ag^{I}$ [28], $Cd^{II}$ [29], $Zn^{II}$ [29–32], $Cu^{I}$ [33–36] and $Fe^{II}$ [37] have previously been reported with 3,5-di-2-pyridyl-1,2,4-triazole and its derivatives. Chen et al. has also summarised the different 1:1 isomeric complexes with $Cu^{I}$ in a tetrahedral coordination environment that can potentially form with this ligand in its deprotonated state [36]. These are chair, [2 × 2] grids, circular helicate, $4_1$ helix, zigzag chain or $2_1$ helix. In the case of ligands **L1** and **L2**, in line with previous studies on closely related ligands [30,38] and also due to the bulkiness of the ferrocene group, we anticipated that the nitrogen of the imine/amide groups and the adjoining nitrogen atom on the triazole were less likely to be coordinated. Therefore, in this study, *cis*-bridging [2 × 2] grids or polymeric helices were the only 1:1 complexes in a tetrahedral coordination environment that could reasonably be expected to form.

In this contribution, we report the facile synthesis and in-depth characterisation of ferrocene-containing ligands **L1** and **L2** (Scheme 1), including X-ray crystallographic studies. Their complexation with the metal ions $Cu^{I}$, $Ag^{I}$, $Zn^{II}$ and $Cd^{II}$, as studied by NMR and UV–vis spectroscopies and by electrochemistry, is also reported.

## 2. Results and discussion

### 2.1. Synthesis and characterisation of ligands

Both ligands *N*-4-[3,5-di-(2-pyridyl)-1,2,4-triazoyl]ferrocene carbimine (**L1**) and *N*-4-[3,5-di-(2-pyridyl)-1,2,4-triazoyl]ferrocene carbamide (**L2**) were obtained in good yields by reacting the known compound 3,5-di-pyridine-2-yl-[1,2,4]triazol-4-ylamine [25,26] (**1**) with the commercially available ferrocenecarbaldehye and the easy-to-prepare chlorocarbonyl ferrocene [39,40] (**2**), respectively (see Scheme 1). Interestingly, both ligands did not need to be purified by column chromatography. The main impurity of **L1**, ferrocencarbaldehyde, could be easily washed away/recovered due to its solubility in hexane. The poor solubility of **L2** in dichloromethane allowed the effective removal of all impurities. The formation of **L1** and **L2** was confirmed unambiguously by $^{1}H$ NMR spectroscopy with, for both ligands, the disappearance of the proton signal of the amine group of **1** at 8.51 ppm and the appearance of the imine proton of **L1** and amide proton of **L2** at 8.71 ppm and 10.84 ppm, respectively. Furthermore, the presence of **L1** and **L2** was further ascertained by $^{13}C$ NMR spectroscopy with two peaks at 173.02 ppm and 170.42 ppm corresponding to the imine carbon of **L1** and the amide carbon of **L2**, respectively.

### 2.2. X-ray crystallography studies [41]

Orange needles of **L1** suitable for X-ray analysis were grown by slow diffusion of ether into a solution of **L1** in dichloromethane. The crystallographic structure of **L1** (see Fig. 1) reveals classical interatomic and torsion angles for such types of bonds [42]. Hence, the average distance between the cation $Fe^{2+}$ and the carbon atoms of the Cp ring (Cp = cyclopentadienyl) of ferrocene is about 2.04 Å and the angle between the two Cp planes is 0.7(2)°. Of interest for the purpose of this work, is the fact that the pyridine rings can rotate to allow the formation of the desired grid-type geometry.

Interestingly, two polymorphs were obtained during our attempts to crystallise **L2**. The first polymorph crystallised in the non-centrosymmetric orthorhombic space group *Fdd2*, with one molecule in the asymmetric unit, Fig. 2. The second crystallized in the centrosymmetric monoclinic space group $P2_1/c$, with two independent molecules per asymmetric unit, Fig. 3. It can be seen that there are significant structural differences between these two polymorphs. In the orthorhombic polymorph the two nitrogen atoms of the pyridine rings, N5 and N6, are oriented on the same side as the two nitrogen atoms of the triazole ring, N3 and N4. There are, therefore, no intramolecular N–H···N hydrogen bonds formed. Interestingly, Fig. 2 shows clearly that ligand **L2** has the ideal geometry to form the [2 × 2] grid-type complex with the two pyridine rings, which are almost co-planar with the triazole ring.

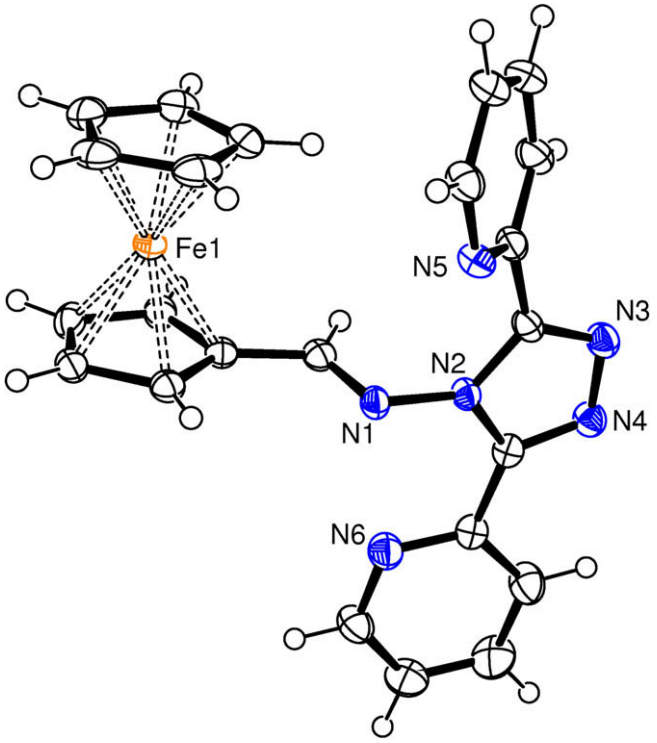


**Fig. 1.** ORTEP plot of **L1**, with thermal ellipsoids drawn at the 50% probability level.

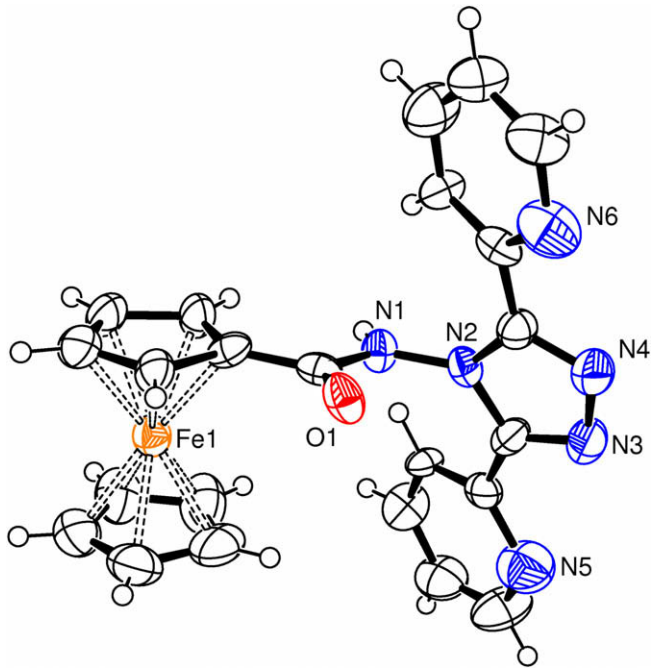


**Fig. 2.** A view of the orthorhombic polymorph of **L2** with thermal ellipsoids drawn at the 50% probability level.

In the monoclinic polymorph the two independent molecules have a slightly different geometry (Fig. 3) with the pyridine rings being orientated differently with the respect to the plane of the pyrazole ring. In the molecule involving Fe1, both pyridine N-atoms, N5 and N6, are oriented in the direction of the nitrogen atom (N1) of the amide group, resulting in the formation of an intramolecular hydrogen bond with the NH group (Table 1). In the molecule involving Fe2, only one of the pyridine N-atoms, N11, faces the nitrogen atom (N7) of the amide group, which hydrogen bonds to atom N4 in the first molecule (Table 1). The two molecules are also connected via an intermolecular hydrogen bond involving the amide (N1) H-atom and pyridine N-atom N12 (Table 1).

**Table 1**
Distances (Å) and angles (°) formed by the H-bonds for the monoclinic polymorph of **L2**. Symmetry operation used to generate the equivalent atoms: (i) = $x, y-1, z$.

| D–H···A | D–H | H···A | D···A | D–H···A |
|---|---|---|---|---|
| N1–H1A···N6 | 0.87(3) | 2.36(3) | 2.806(3) | 112(2) |
| N1–H1A···N12$^{i}$ | 0.87(3) | 2.57(2) | 3.205(2) | 131(3) |
| N7–H7A···N4 | 0.89(2) | 2.26(3) | 3.070(2) | 152(3) |

**Table 2**
Shift in formal potential,[a] $\Delta E^{\circ\prime} = E^{\circ\prime}_{com} - E^{\circ\prime}_{host}$, for the ferrocene-centered redox couple of selected ligand upon the addition of 1.1 equiv. of metallic cations in a mixture of $CH_2Cl_2$:acetonitrile 1:1 V/V at ambient temperature.

| Metal | $E^{\circ\prime}$ (**L1**) (mV) | $E^{\circ\prime}$ (**L2**) (mV) |
|---|---|---|
| $Zn^{II}$ | +51 | +53 |
| $Cu^{I}$ | +41 | +57 |
| $Ag^{I}$ | +39 | +32 |
| $Cd^{II}$ | +45 | +43 |

[a] Formal potentials, $E^{\circ\prime}$, at ambient temperature, referenced to $E^{\circ\prime}$ ($Fc^{0/+}$) as internal reference, were determined as the midpoint between the anodic and cathodic peak potentials $(E_{pa} + E_{pc})/2$; the margin of error was ±5 mV.

### 2.3. Metal-binding studies

All the complexes were made *in situ* by mixing one equivalent of ligand with one equivalent of a metallic salt ($Zn(CF_3SO_3)_2$, $AgPF_6$, $CuPF_6{\cdot}4CH_3CN$ and $CdCl_2$ were used) in $CD_3CN$ (10 mM concentration). The choice of these metal ions was dictated by their diamagnetic nature and their preference for a tetrahedral geometry. The similarity of the $^1H$ NMR spectra when different $Zn^{II}$ salts ($CF_3SO_3^-$, $ClO_4^-$ and $NO_3^-$) were added indicated the lack of different competitive interactions from counter-ions. $^1H$ NMR spectra of **L1**

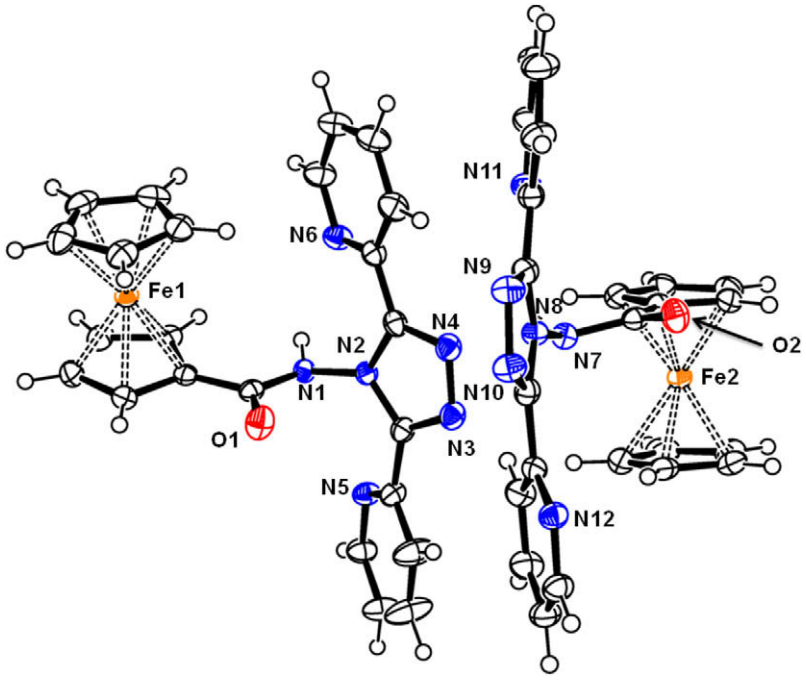


**Fig. 3.** ORTEP plot of the two independent molecules in the monoclinic polymorph of **L2**, with thermal ellipsoids drawn at the 50% probability level.

**Table 3**
Crystallography data for the monoclinic polymorph of **L2**.

| | **L2** – monoclinic polymorph |
|---|---|
| Empirical formula | $C_{23}H_{18}FeN_6O$ |
| $M$ (g mol$^{-1}$) | 450.28 |
| Crystal shape | Block |
| Colour | Orange |
| Crystal system | Monoclinic |
| Space group | P $2_1$/c |
| $a$ (Å) | 9.3188(5) |
| $b$ (Å) | 11.6723(4) |
| $c$ (Å) | 36.798(2) |
| $\alpha$ (°) | 90 |
| $\beta$ (°) | 92.561(5) |
| $\chi$ (°) | 90 |
| $V$ (Å$^3$) | 3998.6(4) |
| $Z$ | 8 |
| $T$ (K) | 153(2) |
| $\lambda$ (Å) | 0.71073 |
| $D_{calc}$ (g cm$^{-3}$) | 1.496 |
| $\mu$(Mo K$\alpha$) (mm$^{-1}$) | 0.783 |
| Number of data measured | 27 379 |
| Unique data ($R_{int}$) | 7318 (0.0604) |
| Observed Data [$I > 2(\sigma)I$] | 6257 |
| Restraints | 0 |
| Number of parameters | 567 |
| Final $R_1$[a], $wR_2$[b] (observed data) | 0.0372, 0.1004 |
| Final $R_1$[a], $wR_2$[b] (all data) | 0.0448, 0.1049 |
| $\rho_{min}$, $\rho_{max}$ (e Å$^{-3}$) | −0.504, 0.733 |

[a] $R_1 = \Sigma||F_o| - |F_c||/\Sigma|F_o|$.
[b] $wR_2 = [\Sigma w(F_o^2 - F_c^2)^2/\Sigma w(F_o^2)^2]^{1/2}$.

and **L2** and their respective Ag$^I$, Zn$^{II}$, Cu$^I$ and Cd$^{II}$ complexes are presented in data Appendix A (Figs. S1 and S2).

It was difficult to obtain better spectra for the Cu$^I$ complex of **L1** and for the Cd$^{II}$ complex of **L2** as these complexes precipitated quickly. However, for all the other complexes, significant shifts of all the ferrocene protons were observed for both these complexes. For all the **L1** complexes, small downfield shifts in the signals for the pyridine and ferrocene protons were observed, with the only exception being the imine proton and the underivatised Cp ring of the Ag$^I$ complex, which underwent a small upfield shift. In addition, the changes were smaller for this complex, probably due to its cation having only one positive charge. Similar results to those obtained for **L1** were found with **L2**, with again the underivatised Cp of the Ag complex being upfield shifted and the pyridine protons of metal complexes generally undertaking a downfield shift. An interesting observation was the shift of the amide proton which was +1.80 ppm for the Ag$^I$ complex, +0.60 ppm for the Zn$^{II}$ complex and +0.60 ppm for the Cu$^I$ complex. If intramolecular H-bonding in **L2**, as indicated in the solid-state from the X-ray measurements, is also present in solution, complexation of the pyridine nitrogens would break this interaction, with downfield shifts then indicating extensive interaction with solvent molecules. IR spectroscopy measurements on **L2** in acetonitrile, which were undertaken to monitor the shifts of the $\nu_{N-H}$ vibration stretch, were compounded by the presence of signals from the solvent. However, no shift in the amide carbonyl stretch was found upon complexation, which, in agreement with previous studies on related ligands [19], suggests that this bond does not play a role in the complexation of these d-block metals.

In order to establish complex stoichiometries, some NMR titration experiments were undertaken by following the shift in the most downfield ferrocene proton signal of **L1** (4.68 ppm) and **L2** (4.78 ppm) (ca. 5 mM, $CD_3CN$) upon addition of aliquots of ligand. The absence of new signals at sub-stoichiometric ratios indicated that exchange between complexed and uncomplexed ligand was fast on the NMR timescale. In the case of Cu$^I$, although downfield shifts were small, it was clear that complexes of 1:1 stoichiometry were forming (see Appendix A for example with **L2**) with no further shifts observed after the addition of more than 1.0 equivalent of the metal ion. A similar result was found in the case of Zn$^{II}$, except that the curve shape indicated that the 1:1 complex formed via a 2:1 (ligand:metal) complex, which was clearly predominant in the presence of half an equivalent of metal ion (see Appendix A for example with **L1**). It might be possible that the coordination of solvent or counter-anion to the Zn$^{II}$ ion might stabilise the formation of an octahedral six-coordinate 2:1 (ligand:metal) complex, a structure that has been previously reported by others [30,38] on 3,5-di-2-pyridyl-1,2,4-triazole derivative ligands. In fact, all the X-ray structures of Zn$^{II}$ complexes reported to date with this ligand system have solvent molecules or counter-anions coordinated to the metal ion [29–32].

As outlined in the introduction, out of the various possible 1:1 geometries [36] with metal ions in a tetrahedral geometry that can form with this ligand, only a [2 × 2] grid structure or a polymer (e.g. a $2_1$ helix) are possible in saturated complexes where both of the heterocyclic binding sites are occupied per ferrocene molecule, as shown schematically in Scheme 2.

In the absence of suitable crystals for X-ray crystallography, mass spectrometry on 1:1 metal:ligand stoichiometry solutions was used to shed further light on the structures of the complexes, which in each case revealed fragments of metal complexes but none at or above the molecular weight of a tetrameric assembly.

In order to get further insight into the complexation process, UV–vis measurements were carried out in a 1:1 v/v $CH_2Cl_2$:acetonitrile mixture to observe the shift of $\lambda_{max}$ of the characteristic d–d band of the ferrocene moiety as well as the change of the absorbance ε upon complexation. In general, changes in $\lambda_{max}$ were small but slightly more marked for **L1** with small bathochromic shifts of up to +30 nm observed (see Table in Appendix A). In addition for **L1**, a general increase in the molar extinction coefficient was more apparent, with a visible change in colour from orange to red observed upon complexation. These results suggest that the conjugated imine linker allows for a slightly better chromogenic response from electronic bands associated with the ferrocene unit.

### 2.4. Electrochemistry

Cyclic voltammetry (CV) was performed on ligands **L1** and **L2** in a 1:1 mixture by volume of $CH_2Cl_2$:MeCN to determine the effect of the complexation on the ferrocene-centered redox couple (see

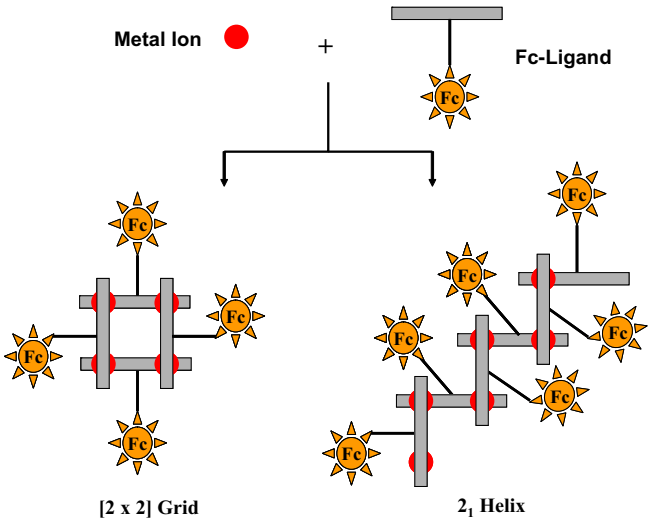


**Scheme 2.** Schematic representation of possible structures which can be obtained with a metal:ligand 1:1 stoichiometry.

Section 4 for further details). Their cyclic voltammograms (CV) all indicated reversible, one-electron transfers, for which the formal potentials, $E^{\circ\prime}$, were determined as $E^{\circ\prime}_{\mathbf{L1}} = 241$ mV and $E^{\circ\prime}_{\mathbf{L2}} = 254$ mV versus $E^{\circ\prime}(Fc^{0/+})$ (Fc = ferrocene, used as internal reference). There was thus little dependence on $E^{\circ\prime}$ by changing the linker group from an imine to an amide.

Electrochemical data for ligands **L1** and **L2** in the presence of 1.1 equiv. of metal cation are presented in Table 2 (see Appendix A for the CV of **L2** in the presence of $Cu^{I}$). All the voltammograms gave one-wave behaviour, demonstrating a gradual positive shift in the ferrocene-centred redox potential upon the addition of increasing amounts of guest. Further additions of metal ion gave no further significant changes, in line with 1:1 complex stoichiometries. As found with the NMR studies, no distinct counter-ion effect was observed in that the addition of 1.1 equiv. of three different salts of $Zn^{II}$ ($CF_3SO_3^-$, $ClO_4^-$ and $NO_3^-$) to a solution of **L1** gave similar $\Delta E^{\circ\prime}$ values within the margin of error (+49, +55 and 51 mV, respectively).

The shifts in electrode potential confirm that complex formation can be followed electrochemically and, in line with previous studies on the complexation of metal ions by ferrocene-containing ligands [19,20,23,24], the positive shifts indicate that the ferrocene centre is harder to oxidise upon complexation due to the effect of the positively charged metal centres lying in relatively close proximity to the redox centre. However, the comparison with previous work [19,20] also suggests that the relatively small potential shifts observed here are consistent with the metal-binding sites being located not directly adjacent to the ferrocene unit but at the heterocyclic units, in agreement with other results presented in this study that point to only the heterocyclic groups being involved in the formation of these 1:1 complexes.

The shifts in potential obtained for both ligands are relatively similar and with the exception of $Cu^{I}$, are within the margin of error. While this supports the notion that complex geometries are similar for both ligands, it also indicates that marginally better electronic communication between the binding site and the ferrocene unit in **L1**, as indicated from the UV–vis studies, does not manifest itself in the electrochemical data. This effect in ferrocene-based systems has been discussed in detail previously [43]. These latest findings presented here indicate that in terms of the electrochemical sensing of metal ions, conjugated C=C links are more effective at communicating binding events than their imine counterparts [19,20].

The positive shifts observed in this study indicate that the complexes are more weakly bound in their oxidised forms, with decreases in binding strength upon oxidation of up to 1 order of magnitude (see Appendix A for further details). Such redox-switched binding [24,44,45] is consistent with our previous work on related H-bonded systems [46,47] and can be explained here on electrostatic grounds. It is interesting to note however that the high electrochemical and chemical reversibilities of the cyclic voltammograms for each system indicate that the complexes remain intact upon ferrocene oxidation under the conditions used in each experiment. This result is not unexpected in that more pronounced changes might only be expected when oxidation encourages phenomena such as intermolecular aggregation [17,18] or ejection of the binding species. The latter process has been observed as a result of oxidation inducing chemical changes to the interacting components [48] or when the binding site for a highly charged guest is located very near to the redox-active unit [49].

## 3. Conclusion

Two new ferrocene-containing ligands (**L1** and **L2**) have been synthesised, fully characterised and their structures proven by X-ray crystallographic analysis. Their complexation with several diamagnetic metal ions has been monitored by a number of analytical methods, with the results of these indicating the formation in solution of 1:1 complexes with grid-like or linear geometries. The presence of the tethered ferrocene group has allowed the complexation process to be followed by electrochemistry, which has indicated that such complexes become more weakly bound but remain intact upon oxidation under the experimental conditions used.

Further studies on other ferrocene-based ligands that can electrochemically sense the formation of complexes with specific geometries are currently underway in our laboratories and will be published in due course.

## 4. Experimental

### 4.1. Materials

All reagents were purchased from commercial suppliers and used as received without further purification. Solvents were used with a technical purity for reactions, or, when mentioned, purified by standard literature methods prior to use [50].

### 4.2. Physical measurements

NMR spectra were recorded on a Brucker AMS 400 FTP spectrometer or on a Bruker Advance DRX 400 MHz spectrometer with different kinds of deuterated solvents. The chemical shifts ($\delta$) were reported in ppm values with the residual solvent peaks used as an internal reference. Coupling constants ($J$) are given in Hertz (Hz). The following abbreviations were used: s (singlet), d (doublet), t (triplet), m (multiplet), and b (broad). NMR titrations were carried out by adding aliquots of a stock solution of the particular metal ion to a solution of the ferrocene ligand, in the same solvent ($CD_3CN$). UV–vis spectra were recorded on a Varian Cary 50 Bio spectrometer. UV−vis titrations were carried out by adding aliquots of a stock solution of the particular metal ion to a solution of the ferrocene ligand, in the same mixture of solvent ($CH_2Cl_2$:acetonitrile 1:1 by volume). The absorbance readings for the UV–vis spectra were adjusted to take into account the dilution of the solution during the course of each experiment. Melting and decomposition points were taken on a Gallenkamp apparatus in open capillaries and are uncorrected. Elementary analyses were performed by the microanalysis service of the pharmaceutical and organic chemistry laboratory of Geneva and the Engineer School of Fribourg. Electron impact mass spectrometry was recorded on a NERMAG RC30-10 system. The electron beam energy used to carry out the EI was 70 eV. ESI-Mass Spectrometry was carried out using a LCQ apparatus of Thermofinnigan, San José, California. The infrared spectra were obtained using a Perkin–Elmer FT-IR 1720X spectrometer with potassium bromide disc containing a trace of the sample. Peaks were labelled with the following abbreviations: br (broad), s (strong), m (medium) and w (weak).

### 4.3. Electrochemistry

Cyclic voltammograms were recorded at 293 K using a BAS 50 W Electrochemical Workstation. The cyclic voltammetry experiments were conducted in a dry nitrogen-purged mixture 1:1 by volume $CH_2Cl_2$:acetonitrile, with tetrabutylammoniumperchlorate (0.1 M) as supporting electrolyte. Pt wire was used as the counter-electrode, with a BAS Pt disc working electrode (3 mm diameter) in combination with a BAS Ag/AgCl (3 M NaCl) reference electrode, separated from the main cell compartment by a salt bridge. The potential scan rate was 50 mV $s^{-1}$.

*Caution*: Although no problems were encountered in this work, metal perchlorate salts and complexes are potentially explosive. They must be handled with special care.

### 4.4. Synthesis

#### 4.4.1. 3,5-Di-(2-pyridyl)-4-amino-1,2,4,5-triazole (**1**)

Compound **1** was synthesised following the procedure reported by Geldard and Lions [51]. The analytical data of the obtained product matched that reported by Brooker and co-workers [30].

#### 4.4.2. N-4-[3,5-di-(2-pyridyl)-1,2,4-triazoyl]ferrocene carbimine (**L1**)

A mixture of ferrocenecarbaldehyde (2.52 g, 11.75 mmol), **1** (2.11 g, 8.84 mmol) and 5 Å molecular sieves (3.50 g) in anhydrous toluene (210 ml) were heated to reflux in a three-necked flask equipped with a magnetic stirring bar and a reflux condenser, under an atmosphere of nitrogen. When the reflux started, 10 drops of sulphuric acid 96% were added to the mixture. Every hour, 10 supplementary drops were added until all of **1** had been converted (NMR-analysis). After a further 22 h stirring, the reaction was cooled to room temperature and filtered on celite. The residue of filtration was then washed with toluene (70 ml). A rapid washing of the organic phase with water (210 ml) was carried out to remove any excess sulphuric acid. After evaporation to dryness, the orange-red residual solid was washed with hexane (3 × 70 ml) to remove the excess ferrocenecarbaldehyde. Finally a red solid was obtained. The slow diffusion of ether into a solution of pure **L1** in dichloromethane, in a 16 mm glass tube, after approximately two days under a nitrogen atmosphere, gave red block-like crystals suitable for X-ray analysis. Yield: 2.15 g (56%); m.p.: 194 °C (decomp.). $^1$H NMR ($CD_3CN$, $\delta$): 4.23 (s, 5H, C*H* Cp), 4.58 (m, 2H, C*H* Cp), 4.70 (m, 2H, C*H* Cp), 7.47 (ddd, 2H, $^3J$ = 7.8 Hz, $^3J$ = 4.8 Hz, $^4J$ = 1.2 Hz, C*H* pyridyl), 7.93 (ddd, 2H, $^3J$ = 7.8 Hz, $^4J$ = 1.8 Hz, C*H* pyridyl), 8.10 (ddd, 2H, $^3J$ = 7.8 Hz, $^5J$ = 1.0 Hz, C*H* pyridyl), 8.59 (s, 1H, N=C*H*), 8.66 (ddd, 2H, $^3J$ = 4.8 Hz, $^4J$ = 1.8 Hz, $^5J$ = 1.0 Hz, C*H* pyridyl). $^{13}$C NMR ($CDCl_3$, $\delta$): 70.00 (*C*H Cp), 72.57 (*C*H Cp), 74.99 (*C*H Cp), 77.62 (*C* Cp), 124.57 (*C*H pyridyl), 125.19 (*C*H pyridyl), 137.11 (*C*H pyridyl), 147.47 (*C* pyridyl), 149.64 (*C*H pyridyl), 151.01 (*C* triazole), 173.02 (N=*C*H). ESI-MS *m/z*: 457 ([M+Na]$^+$), 435 ([M+H]$^+$). IR (KBR disc): 3425m, 3118w, 3082m, 2923m, 2853w, 1678w, 1601s, 1584s, 1566m, 1522w, 1473m, 1450s, 1429s, 1394m, 1365m, 1350m, 1281w, 1257m, 1206w, 1181w, 1147m, 1105m, 1092m, 1044m, 1034m, 994m, 976w, 899w, 821m, 791s, 740m, 716m, 700m, 670w, 647w, 619w, 599m, 520m, 502m, 461w, 403w. Anal. Calc. for $FeC_{23}H_{18}N_6{\cdot}0.5H_2O$: C, 62.32; H, 4.32; N, 18.96. Found: C, 62.53; H, 4.09; N, 19.05%.

#### 4.4.3. Chlorocarbonylferrocene (**2**)

Compound **2** was synthesised following the procedure published by Wende and co-workers [40] and was used without further purification for the next synthetic step.

#### 4.4.4. N-4-[3,5-di-(2-pyridyl)-1,2,4-triazoyl]ferrocene carbamide (**L2**)

A solution of **2** (0.61 g, 2.45 mmol), in anhydrous dichloromethane (120 ml), was added dropwise at 0 °C over a period of 90 min from a funnel tube, onto a mixture of triethylamine (0.27 g, 2.69 mmol), **1** (0.64 g, 2.69 mmol) and anhydrous dichloromethane (20 ml) in a 250 ml two-necked flask equipped with a magnetic stirring bar. The reaction was allowed to return to room temperature and stirred for 64 h. The reaction was quenched with saturated $NaHCO_3$ (90 ml) and the aqueous layer was extracted with dichloromethane (3 × 150 ml). The combined extracts were dried ($MgSO_4$), filtered and the solvent removed under reduced pressure to give an orange solid. This solid was washed with dichloromethane (3 × 5 ml) to obtain pure **L2** as an orange solid. The slow diffusion of ether into a solution of pure **L2** in dichloromethane in a 16 mm glass tube, gave, after about three days under a nitrogen atmosphere, orange block-like crystals suitable for X-ray analysis. Yield: 0.65 g (59%); m.p.: 221 °C (decomp.). $^1$H NMR ($CD_3CN$, $\delta$): 4.10 (s, 5H, C*H* Cp), 4.45 (m, 2H, C*H* Cp), 4.77 (m, 2H, C*H* Cp), 7.46 (ddd, 2H, $^3J$ = 7.8 Hz, $^3J$ = 4.9 Hz, $^4J$ = 1.2 Hz,), 7.96 (ddd, 2H, $^3J$ = 7.8 Hz, $^4J$ = 1.7 Hz, *H* pyridyl), 8.18 (ddd, 2H, $^3J$ = 7.8 Hz, $^5J$ = 1.0 Hz, *H* pyridyl), 8.70 (ddd, 2H, $^3J$ = 4.9 Hz, $^4J$ = 1.7, $^5J$ = 1.0 Hz, *H* pyridyl), 10.10 (s, 1H, N*H*). $^{13}$C NMR ($CDCl_3$, $\delta$): 69.08 (*C*H Cp), 70.43 (*C*H Cp), 71.88 (*C*H Cp), 77.63 (*C* Cp), 124.51 (*C*H pyridyl), 125.08 (*C*H pyridyl), 137.85 (*C*H pyridyl), 147.36 (*C* pyridyl), 149.22 (*C*H pyridyl), 152.07 (C triazole), 170.42 (CO). ESI-MS *m/z*: 449 ([M−H]$^-$). IR (KBR disc): 3256m, 3081m, 3006w, 1690s, 1677s, 1588m, 1569m, 1537m, 1520m, 1498m, 1476m, 1467m, 1446s, 1412m, 1375m, 1354w, 1312w, 1292m, 1279s, 1223w, 1180w, 1156m, 1125m, 1092m, 1052w, 1034w, 1010w, 994m, 971w, 928w, 876w, 843w, 823m, 792s, 770w, 754w, 739m, 702m, 634w, 621w, 608m, 531w, 498m, 482m, 457w, 404w. Anal. Calc. for $FeC_{23}H_{18}N_6O{\cdot}0.5H_2O$: C, 60.15; H, 4.17; N, 18.30. Found: C, 60.44; H, 3.90; N, 18.45%.

#### 4.4.5. Synthesis of complexes with **L1** and **L2**

Complexes were made *in situ* by addition of the metal salt in acetonitrile to the ligand in acetonitrile. The triflate or perchlorate hexahydrate salts for $Zn^{II}$, the hexafluorophosphate salt for $Ag^{I}$, the chloride salt for $Cd^{II}$ and the tetrakis(acetonitrile)hexafluorophosphate salt for Cu(I), were used as they are relatively soluble in this solvent.

*4.4.5.1. $Zn^{II}$ complex with **L1**.* $^1$H NMR ($CD_3CN$, $\delta$): 4.29 (s, b, 5H, Cp*H*), 4.82 (s, b, 2H, Cp*H*), 4.96 (m, b, 2H, Cp*H*), 7.82 (m, b, 2H, *H* pyridyl), 8.30 (m, b, 2H, *H* pyridyl), 8.38 (m, b, 2H, *H* pyridyl), 8.77 (m, b, 3H, C*H*=N and *H* pyridyl).

*4.4.5.2. $Ag^{I}$ complex with **L1**.* $^1$H NMR ($CD_3CN$, $\delta$): 4.18 (s, b, 5H, Cp*H*), 4.73 (m, b, 2H, Cp*H*), 4.87 (m, 2H, Cp*H*), 7.62 (m, 2H, *H* pyridyl), 8.08 (m, b, 2H, *H* pyridyl), 8.21 (m, b, 2H, *H* pyridyl), 8.54 (s, b, 1H, N=C*H*), 8.78 (m, b, 2H, *H* pyridyl).

*4.4.5.3. $Cd^{II}$ complex with **L1**.* $^1$H NMR ($CD_3CN$, $\delta$): 4.28 (s, b, 5H, Cp*H*), 4.79 (m, b, 2H, Cp*H*), 4.94 (m, b, 2H, Cp*H*), 7.74 (m, b, 2H, *H* pyridyl), 8.24 (m, b, 2H, *H* pyridyl), 8.39 (m, b, 2H, *H* pyridyl), 8.76 (s, b, 1H, N=C*H*), 8.83 (m, b, 2H, *H* pyridyl).

*4.4.5.4. $Zn^{II}$ complex with **L2**.* $^1$H NMR ($CD_3CN$, $\delta$): 4.20 (s, b, 5H, Cp*H*), 4.68 (m, b, 2H, Cp*H*), 5.00 (m, b, 2H, Cp*H*), 7.80 (m, b, 2H, *H* pyridyl), 8.24 (m, b, 2H, *H* pyridyl), 8.40 (m, b, 2H, *H* pyridyl), 8.82 (s, b, 2H, *H* pyridyl), 10.71 (s, b, 1H, CON*H*).

*4.4.5.5. $Ag^{I}$ complex with **L2**.* $^1$H NMR ($CD_3CN$, $\delta$): 3.95 (s, b, 5H, Cp*H*), 4.50 (m, b, 2H, Cp*H*), 4.89 (m, b, 2H, Cp*H*), 7.52 (m, b, 2H, *H* pyridyl), 7.97 (m, b, 2H, *H* pyridyl), 8.18 (m, b, 2H, *H* pyridyl), 8.63 (m, b, 2H, *H* pyridyl), 11.88 (s, b, 1H, CON*H*).

*4.4.5.6. $Cu^{I}$ complex with **L2**.* $^1$H NMR ($CD_3CN$, $\delta$): 4.17 (s, b, 5H, Cp*H*), 4.65 (m, b, 2H, Cp*H*), 4.99 (m, b, 2H, Cp*H*), 7.78 (m, b, 2H, *H* pyridyl), 8.21 (m, b, 2H, *H* pyridyl), 8.39 (m, b, 2H, *H* pyridyl), 8.80 (m, b, 2H, *H* pyridyl), 10.69 (s, b, 1H, CON*H*).

### 4.5. X-ray crystallography analysis

Intensity data for the monoclinic polymorphs of **L2** were collected using a STOE Image Plate Diffraction System with graphite monochromated Mo Kα radiation ($\lambda$ = 0.71073 Å). The structure was solved by Direct methods using the program SHELXS-97 [52]. The refinement and all further calculations were carried out using SHELXL-97 [52]. The NH and $NH_2$ H-atoms were located from

difference Fourier maps and freely refined. The C-bound H-atoms were included in calculated positions and treated as riding atoms using SHELXL default parameters. The non-H atoms were refined anisotropically, using weighted full-matrix least-squares on $F^2$. Multi-scan absorption corrections were applied using the MULscanABS routine in PLATON [53]. Crystallographic data and refinement details are summarised in Table 3. The figures are drawn using the program PLATON [53].

## Acknowledgements

This work was partially supported by the Swiss National Science Foundation (SNFS), l'Etat de Neuchâtel and the Erasmus Exchange Programme.

## Appendix A. Supplementary material

CCDC 668662, 216247 and 730636 contain the supplementary crystallographic data for compounds **L1**, **L2** (orthorhombic polymorph) and **L2** (monoclinic polymorph). These data can be obtained free of charge from The Cambridge Crystallographic Data Centre via http://www.ccdc.cam.ac.uk/data_request/cif.

Supplementary data associated with this article can be found, in the online version, at doi:10.1016/j.jorganchem.2009.10.004.

## References

[1] J.A. Thomas, Chem. Soc. Rev. 36 (2007) 856–868. and references therein.
[2] C.P. Pradeep, D.-L. Long, G.N. Newton, Y.-F. Song, L. Cronin, Angew. Chem., Int. Ed. 47 (2008) 4388–4391. and references therein.
[3] J.-M. Lehn Supramolecular Chemistry: Concepts and Perspectives, Wiley-VCH, Weinheim, Germany, 1995 (Chapter 9).
[4] M. Ruben, J. Rojo, F.J. Romero-Salguero, L.H. Uppadine, J.-M. Lehn, Angew. Chem., Int. Ed. 43 (2004) 3644–3662. and references therein.
[5] G.F. Swiegers, T.J. Malhefetse, Chem. Rev. 100 (2000) 3483–3537. and references therein.
[6] J.R. Nitschke, M. Hutin, G. Bernardinelli, Angew. Chem., Int. Ed. 43 (2004) 6724–6727. and references therein.
[7] L.H. Uppadine, J.-P. Gisselbrecht, N. Kyritsakas, K. Nättinen, K. Rissanen, J.-M. Lehn, Chem. Eur. J. 11 (2005) 2549–2565. and references therein.
[8] D.M. Bassani, J.-M. Lehn, S. Serroni, F. Puntoriero, S. Campagna, Chem. Eur. J. 9 (2003) 5936–5946. and references therein.
[9] M.S. Alam, S. Strömdörfer, V. Dremov, P. Müller, J. Kortus, M. Ruben, J.-M. Lehn, Angew. Chem., Int. Ed. 44 (2005) 7896–7900. and references therein.
[10] K.L. Thomson, Coord. Chem. Rev. 233/234 (2002) 193–206.
[11] D.S. Cati, J. Ribas, J. Ribas-Arino, H. Stoeckli-Evans, Inorg. Chem. 43 (2004) 1021–1030. and references therein.
[12] L.N. Dawe, L.K. Thompson, Angew. Chem., Int. Ed. 46 (2007) 7440–7444.
[13] C.L. Hill, X. Zhang, Nature 373 (1995) 324.
[14] A. Harriman, R. Ziessel, J.-C. Moutet, E. Saint-Aman, Phys. Chem. Chem. Phys. 5 (2003) 1593–1598.
[15] E.C. Constable, R. Martínez-Máñez, A.M.W. Cargill Thompson, J.V.J. Walker, Chem. Soc., Dalton Trans. (1994) 1585–1594.
[16] H.-B. Yang, K. Ghosh, Y. Zhao, B.H. Northrop, M.M. Lyndon, D.C. Muddiman, H.S. White, P.J. Stang, J. Am. Chem. Soc. 130 (2008) 839–841.
[17] K. Tsuchiya, H. Sakai, T. Saji, M. Abe, Langmuir 19 (2003) 9343–9350. and references therein.
[18] J.C. Medina, I. Gay, Z.H. Chen, L. Echegoyen, G.W. Gokel, J. Am. Chem. Soc. 113 (1991) 365–366.
[19] J.D. Carr, S.J. Coles, M.B. Hursthouse, J.H.R. Tucker, J. Organomet. Chem. 637–639 (2001) 304–310.
[20] J.D. Carr, S.J. Coles, M.B. Hursthouse, M.E. Light, E.L. Munro, J.H.R. Tucker, J. Westwood, Organometallics 19 (2000) 3312–3315.
[21] L.A. Levine, S.I. Kirin, C.P. Myers, S.A. Showalter, M.E. Williams, Eur. J. Inorg. Chem. (2009) 613–621.
[22] J.E. Aguado, O. Crespo, M. Concepción Gimeno, P.G. Jones, A. Laguna, Y. Nieto, Eur. J. Inorg. Chem. (2008) 3031–3038.
[23] N. Sadhukhan, J.K. Bera, Inorg. Chem. 48 (2009) 978–990.
[24] P. Molina, A. Tárraga, A. Caballero, Eur. J. Inorg. Chem. 22 (2008) 3401–3417. and references therein.
[25] M.A. Withersby, A.J. Blake, N.R. Champness, P.A. Cooke, P. Hubberstey, W.-A. Li, M. Schröder, Inorg. Chem. 38 (1999) 2259.
[26] J.F. Geldard, F. Lions, J. Org. Chem. 30 (1965) 318.
[27] M.T. Youinou, N. Rahmouni, J. Fischer, J.A. Osborn, Angew. Chem., Int. Ed. Engl. 31 (1992) 733.
[28] S.C. Shao, Z.L. You, S.P. Zhang, S.W. Ng, H.L. Zhu, Acta Crystallogr., Sect. E: Struct. Rep. Online E61 (2005) m265–m267.
[29] Q.-G. Zhai, X.-Y. Wu, S.-M. Chen, C.-Z. Lu, W.-B. Yang, Cryst. Growth Des. 6 (2006) 2126–2135.
[30] M.H. Klingele, P.D.W. Boyd, B. Moubaraki, K.S. Murray, S. Brooker, Eur. J. Inorg. Chem. 3 (2006) 573–589.
[31] M.H. Klingele, A. Noble, P.D.W. Boyd, S. Brooker, Polyhedron 26 (2007) 479–485.
[32] U. Hartmann, H. Vahrenkamp, Inorg. Chim. Acta 239 (1995) 13–17.
[33] L. Cheng, W.-X. Zhang, B.-H. Ye, J.-B. Lin, X.-M. Chen, Inorg. Chem. 46 (2007) 1135–1143.
[34] W.-J. Wang, C.-H. Lin, J.-S. Wang, S.-W. Tang, Mol. Cryst. Liq. Cryst. 456 (2006) 209–219.
[35] J.-P. Zhang, Y.-Y. Lin, X.-C. Huang, X.-M.J. Chen, Am. Chem. Soc. 127 (2005) 5495–5506.
[36] J.-P. Zhang, Y.-Y. Lin, X.-C. Huang, X.-M. Chen, Chem. Commun. 10 (2005) 1258–1260.
[37] J.A. Kitchen, S. Brooker, Coord. Chem. Rev. 252 (2008) 2072–2092.
[38] U. García-Couceiro, O. Castillo, A. Luque, G. Beobide, P. Román, Acta Cryst. E60 (2004) m720–m722.
[39] S. Arimoto, A.C.J. Haven Jr., Am. Chem. Soc. 77 (1955) 6295–6297.
[40] H.J. Lorkowski, R. Pannier, A.J. Wende, Prakt. Chem. 35 (1967) 149–158.
[41] Note that the X-ray crystal structures of **L1** and the orthorhombic polymorph of **L2** were already deposited in 2003 by our group in the CCDC databank. However, these structures have never been reported in context.
[42] F.H. Allen, O. Kennard, D.G. Watson, L. Brammer, A.G. Orpen, R. Taylor, J. Chem. Soc., Perkin Trans. 2 (1987) S119.
[43] J.D. Carr, S.J. Coles, W.W. Hassan, M.B. Hursthouse, K.M. Abdul Malik, J.H.R.J. Tucker, Chem. Soc., Dalton Trans. (1999) 57–62.
[44] J.H.R. Tucker, S.R. Collinson, Chem. Soc. Rev. 31 (2002) 147–156.
[45] P.D. Beer, P.A. Gale, G.Z.J. Chen, Chem. Soc., Dalton Trans. 12 (1999) 1897–1910.
[46] H. Miyaji, G. Gasser, S.J. Green, Y. Molard, S.M. Strawbridge, J.H.R. Tucker, Chem. Commun. (2005) 5355–5357.
[47] J. Westwood, S.J. Coles, S.R. Collinson, G. Gasser, S.J. Green, M.B. Hursthouse, M.E. Light, J.H.R. Tucker, Organometallics 5 (2004) 946–951.
[48] S.M. Strawbridge, S.J. Green, J.H.R. Tucker, Chem. Commun. 23 (2000) 2393–2394.
[49] C.D. Hall, N.W. Sharpe, I.P. Danks, Y.P. Sang, J. Chem. Soc., Chem. Commun. 7 (1989) 419–421.
[50] W.L.F. Armarego, D.D. Perrin, Purification of Laboratory Chemicals, fourth ed., Butterworth-Heinemann, Oxford (UK), 1996.
[51] J.F. Geldard, F. Lions, J. Org. Chem. 1965 (1965) 30.
[52] G.M. Sheldrick, Acta Cryst. A64 (2008) 112–122.
[53] A.L. Spek, Acta Cryst. D65 (2009) 148–155.